

Lawrence Berkeley National Laboratory

Lawrence Berkeley National Laboratory

Title

Comparison of Al_xGa_{1-x}N films grown on sapphire by MBE under N-rich and Ga-rich conditions

Permalink

<https://escholarship.org/uc/item/3td2t46h>

Authors

Jasinski, J.
Liliental-Weber, Z.
He, L.
et al.

Publication Date

2002-10-15

Peer reviewed

COMPARISON OF $\text{Al}_x\text{Ga}_{1-x}\text{N}$ FILMS GROWN ON SAPPHIRE BY MBE UNDER N-RICH AND Ga-RICH CONDITIONS

J. JASINSKI, Z. LILIENTAL-WEBER

Lawrence Berkeley National Laboratory, Berkeley, CA 94720, USA

E-mail: jbjasinski@lbl.gov

L. HE, M. A. RESHCHIKOV, H. MORKOÇ

Virginia Commonwealth University, Richmond, VA 23284, USA

E-mail: hmorkoc@vcu.edu

$\text{Al}_x\text{Ga}_{1-x}\text{N}$ layers grown under N-rich and Ga-rich conditions were investigated using transmission electron microscopy (TEM) and photoluminescence (PL). Despite a high density of threading dislocations ($\sim 10^{10} \text{ cm}^{-2}$) these layers had high PL quantum efficiencies. Both, TEM and PL studies showed significant differences between layers grown under N- and Ga-rich conditions. The results indicate that edge dislocations do contribute to nonradiative recombination in $\text{Al}_x\text{Ga}_{1-x}\text{N}$ layers.

1. Introduction

$\text{Al}_x\text{Ga}_{1-x}\text{N}$ attracts a lot of scientific interest due to its potential applications in opto-electronic devices and in high-temperature, high-power and high-frequency electronic devices.[1-2] However, despite the fact that $\text{Al}_x\text{Ga}_{1-x}\text{N}$ layers are commonly used in such devices, there are still problems related with this material, which need to be understood and solved in order to better control its technology and understand its properties. Factors influencing the properties of $\text{Al}_x\text{Ga}_{1-x}\text{N}$ include: strain associated with the lattice and thermal mismatch in heteroepitaxial growth (which results in dislocation formation), alloying effects (which can result in compositional fluctuations, ordering or phase separation) and growth conditions.[2-4] In this paper we compare structural and optical properties of $\text{Al}_x\text{Ga}_{1-x}\text{N}$ layers (with low Al content) grown under N-rich and Ga-rich conditions.

2. Experimental

$\text{Al}_x\text{Ga}_{1-x}\text{N}$ layers with nominal thickness in the range 0.5-1 μm and Al mole fraction, x , in the range of 0.10 – 0.25 were grown on (0001) sapphire substrates by plasma-assisted molecular beam epitaxy (MBE). The layers were grown under either Ga- or N-rich conditions. In the former case, the Al mole fraction was controlled by fixing the Al and Ga source temperatures and varying the N flow for changing the composition, x [5]. In the latter case, x was changed by varying the Ga or Al flux or both, in an overabundant N flux. The value of x in the $\text{Al}_x\text{Ga}_{1-x}\text{N}$ epilayers was evaluated from the peak separation between GaN and AlGaN peaks in X-ray diffraction curves, assuming that the variation of the lattice parameter c between GaN and AlN is proportional to the aluminum mole fraction (Vegard's law).

Transmission electron microscopy (TEM) was used to characterize defects and microstructure of both types of layers. Cross-sectional TEM specimens were prepared by a standard method of mechanical pre-thinning followed by Ar-ion milling and were studied using a TOPCON 002B microscope, operated at 200 kV acceleration voltage. All layers were also investigated by photoluminescence (PL). The steady-state PL was excited either with a He-Cd laser (325 nm) or with a third harmonic of the Ti-sapphire laser (245 nm), dispersed by a 1200 rules/mm grating in a 0.5 m monochromator and detected by a photo multiplier tube.

3. Results and Discussion

TEM results of a typical layer grown under N-rich conditions are shown in Figs 1(a)-1(c). The dominant defects present in these layers were dislocations threading through the layer [Fig. 1(a)]. Bright-field images recorded under multi-beam conditions, for which all types of dislocations are visible, were used to estimate their density. In layers grown under N-rich conditions the density of dislocations in the vicinity of the substrate was $\sim 5 \times 10^{10} \text{ cm}^{-2}$ and decreased with increase of the distance from the substrate reaching the value $\sim 2 \times 10^{10} \text{ cm}^{-2}$ at the layer surface. In order to estimate relative distribution of different types of dislocations (edge, screw and mixed), bright-field images were recorded under two beam conditions for g-vectors parallel to [0002] and [11 $\bar{2}$ 0] directions, respectively. These images are shown in Fig. 1. In images recorded for a g-vector parallel to [0002] edge dislocations are out of contrast, whereas screw dislocations are out of contrast in images recorded for a g-vector parallel to the [11 $\bar{2}$ 0] direction. Mixed-type dislocations appear in both images. In the case of layers grown under N-rich conditions a majority (~95 %) of all dislocations were out of contrast in images recorded for a g-vector parallel to [0002] meaning that they were pure edge-type.

Microstructure and defect distribution in layers grown under Ga-rich conditions differed significantly. First, these layers had a rough surface compared to the layers grown under N-rich conditions [see Fig. 1(d)]. Moreover, despite similar densities of threading dislocations in the layers grown under Ga-rich conditions ($7-8 \times 10^{10} \text{ cm}^{-2}$ in the vicinity of the substrate and $\sim 5 \times 10^9 \text{ cm}^{-2}$ at the layer surface) to those for layers grown under N-rich conditions, the relative densities of different types of dislocations differed in these two types of layers. In the layers grown under Ga-rich conditions edge dislocations were again in the majority (~70 %). However other dislocations were also present in significant densities [see Figs 1(e)-1(f)].

These differences between microstructures of layers grown under N- and metal-rich conditions are not related to growth polarity. Convergent beam electron diffraction (CBED) technique showed that all layers had the same, Ga-polarity.

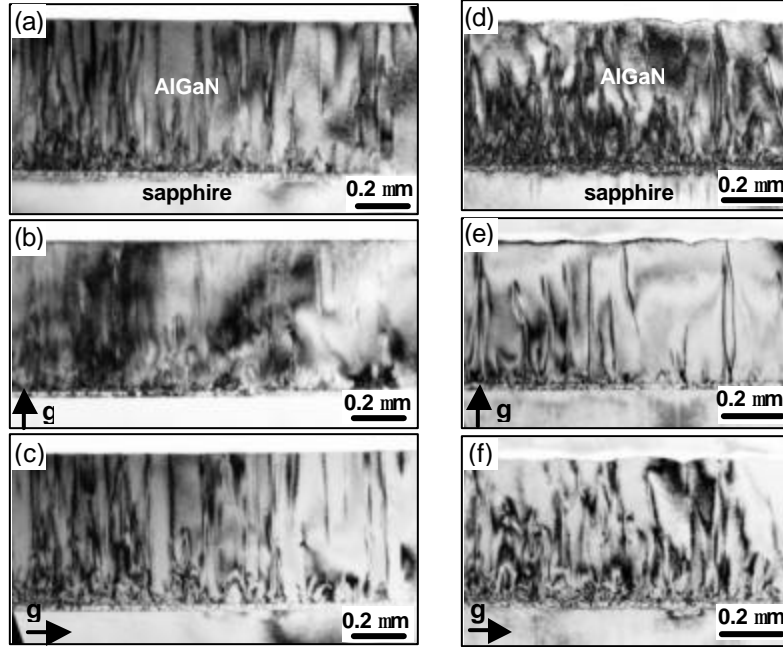


Fig.1. TEM Bright-field images of layers grown under N-rich [(a),(b),(c)] and Ga-rich [(d),(e),(f)] conditions recorded under: (a)/(d) multi-beam condition, (b)/(e) two-beam condition with g -vector parallel to $[0002]$ direction and (c)/(f) two-beam condition with g -vector parallel to $[11\bar{2}0]$ direction.

Figures 2 and 3 show typical PL spectra at different temperatures for the $\text{Al}_x\text{Ga}_{1-x}\text{N}$ samples grown under Ga- and N-rich conditions, respectively. PL spectra of all the $\text{Al}_x\text{Ga}_{1-x}\text{N}$ layers grown under Ga-rich conditions had relatively broad near-band-edge emission peaks and defect-related bands in green and blue regions at low temperatures. The width of the main peak decreased with increasing temperature due to fast quenching at its high-energy side: the full width at half maximum (FWHM) decreased from 93 to 63 meV in the temperature range between 15 and 100 K for the sample depicted in Fig. 2. The narrowing of the emission peak with temperature can be attributed to thermal release of free carriers from the shallower short-range wells and their percolation into the deeper ones caused by local compositional fluctuations in $\text{Al}_x\text{Ga}_{1-x}\text{N}$.

Low-temperature PL spectra of the $\text{Al}_x\text{Ga}_{1-x}\text{N}$ layers grown under N-rich conditions usually contained a relatively sharp near-band-edge emission peak (FWHM is about 40 meV) followed by several LO phonon replicas, as shown in Fig. 3. With increasing temperature the main peak gradually broadened and merged with the phonon replicas.

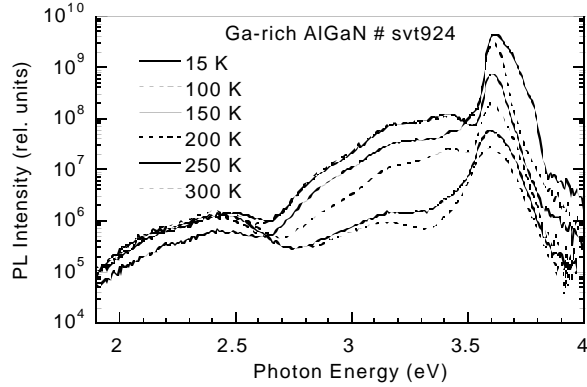


Fig.2. PL spectra of $Al_xGa_{1-x}N$ layer with $x = 0.13$ grown under Ga-rich conditions.

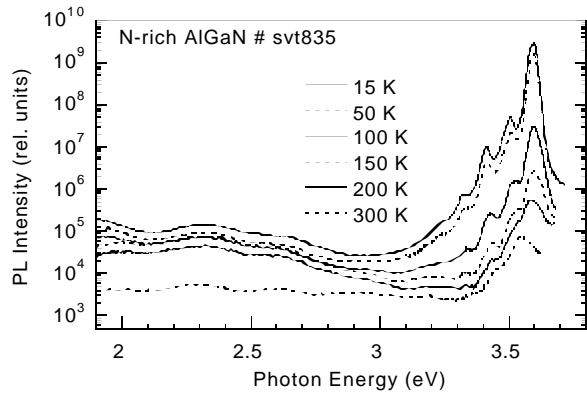


Fig.3. PL spectra of $Al_xGa_{1-x}N$ layer with $x = 0.10$ grown under N-rich conditions.

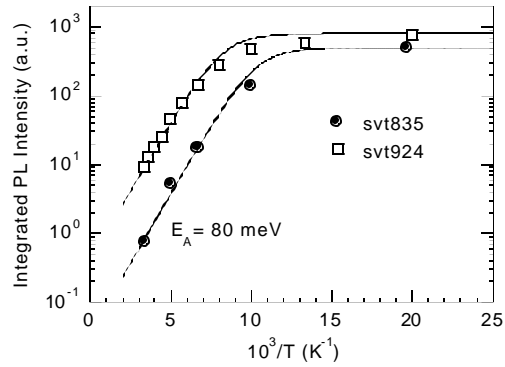


Fig.4. Temperature dependence of the integrated PL intensity for the $Al_xGa_{1-x}N$ layers grown under Ga- (sample svt924) and N-rich (sample svt835) conditions.

The low-temperature quantum efficiency of PL from the layers grown under Ga-rich conditions was several times higher than for the layers grown under N-rich conditions. In particular, for the samples depicted in Figs. 2 and 3, it was 48 % and 10 %, respectively. With increasing temperature the integrated PL intensity quenched with the same activation energy, about 80 meV, for layers grown under Ga - and N-rich conditions, however the quenching of PL from the latter started at lower temperatures (Fig. 4).

Dislocations are believed to act as nonradiative recombination centers in GaN [6-8]. However there is controversy concerning the question as to whether any particular type of dislocation is or is not a nonradiative defect. From comparison of PL intensities for GaN layers with 3 types of dislocations determined by TEM, Hino *et al.* [6] concluded that dislocations with a screw component, screw and mixed dislocations, do act as nonradiative centers in GaN, while edge dislocations do not. In contrast, Cherns *et al.* [7] concluded from comparison of TEM and cathodoluminescence images that threading edge dislocations did act as nonradiative recombination centers in InGaN/GaN quantum wells. Finally Sugahara *et al.* [8] from similar experiments concluded that both pure edge and mixed (screw/edge) dislocations act as nonradiative recombination centers in GaN. Our PL results are consistent with the assumption that the $\text{Al}_x\text{Ga}_{1-x}\text{N}$ layers grown under N-rich conditions contained a higher concentration of nonradiative recombination centers (lower quantum efficiency and quenching starting at lower temperatures) compared to the layers grown under Ga-rich conditions. From the TEM analysis we have estimated that the density of screw and mixed dislocations is comparable in the samples grown under Ga- and N-rich conditions, whereas the density of edge dislocations is much higher in the sample grown under N-rich conditions [about $2 \times 10^{10} \text{ cm}^{-2}$ versus $(3-4) \times 10^9 \text{ cm}^{-2}$ near the sample surface where the PL signal was detected]. Comparison of the PL quantum efficiency with the densities of dislocations in our samples suggests that edge dislocations do act as nonradiative recombination centers in AlGaIn. However, our results do not clearly show whether or not dislocations of the other types contribute to the nonradiative recombination.

It is surprising that such a high density of dislocations as $5 \times 10^9 \text{ cm}^{-2}$ only reduces radiative efficiency by a factor of 2 compared to the expectation of Sugahara *et al.* [8] that there should be a 10 times decrease of PL intensity for a dislocation density in the range $10^9 - 10^{10} \text{ cm}^{-2}$ in GaN. Our results are also contrary to those of Hino *et al.* [6] in that a 10^8 cm^{-2} density of screw and mixed dislocations causes a factor of 5 reduction of PL intensity in GaN. There are several possible explanations reasons for such discrepancies. First, a dislocation density obtained by counting etch-pits and analyzing only plan-view TEM images [6,8] may be underestimated. Moreover, PL intensity may decrease due to other channels of nonradiative recombination, such as deep point defect levels and surface recombination, and relative PL intensities from different samples

studied in Refs. [6] and [7] may not be proportional to their absolute radiative efficiencies.

3. Summary and Conclusions

Structural and optical studies showed significant differences between $\text{Al}_x\text{Ga}_{1-x}\text{N}$ layers grown under N- and Ga-rich conditions. PL peaks in the spectrum measured for layers grown under Ga-rich conditions are broader than those for layers grown under N-rich conditions indicating larger composition fluctuations. On the other hand, significantly higher PL efficiency and its higher thermal stability suggest that there is a lower concentration of non-radiative recombination defects in layers grown under Ga-rich conditions. TEM study shows that both types of layers contain a high density (of the order of 10^{10} cm^{-2}) of threading dislocations however there are significant differences in their distribution among the different types (edge, screw and mixed). The comparison of PL quantum efficiency with these dislocations supports the conclusion that edge-type dislocations do cause nonradiative recombination.

Acknowledgments

This work was supported by the Air Force Office of Scientific Research, through the U.S. Department of Energy under Order No. AFOSR-ISSA-00-0011 (Wood-Witt program). The VCU part of this program was funded by grants from AFOSR, ONR, and NSF. J.J. and Z. L.-W. would like to thank Prof. J. Washburn for fruitful discussions and National Center for Electron Microscopy at LBNL for the opportunity to use its facilities.

References

- [1] J. A. Smart, A. T. Schremer, N. G. Weimann, O. Ambacher, L. F. Eastman, and J. R. Shealy, *Appl. Phys. Lett.* **75**, 388 (1999).
- [2] L. Chang, S.K. Lai, F.R. Chen and J.J. Kai, *Appl. Phys. Lett.* **79**, 928 (2001).
- [3] E. Iliopoulos, K.F. Ludwig, Jr., T.D. Moustakas, S.N.G. Chu, *Appl. Phys. Lett.* **78**, 463 (2001).
- [4] P. Vennegues and H. Lahreche, *Appl. Phys. Lett.* **77**, 4310 (2000).
- [5] L. He, M. A. Reshchikov, F. Yun, D. Huang, and H. Morkoç, *APL* **81**, No. 11, in press (2002).
- [6] T. Hino, S. Tomiya, T. Miyajima, K. Yanashima, S. Hashimoto, and M. Ikeda, *Appl. Phys. Lett.* **76**, 3421 (2000).
- [7] D. Cherns, S. J. Henley, and F. A. Ponce, *Appl. Phys. Lett.* **78**, 2691 (2001).
- [8] T. Sugahara, H. Sato, M. Hao, Y. Naoi, S. Kurai, S. Tottori, K. Yamashita, K. Nishino, L. T. Romano, and S. Sakai, *Jpn. J. Appl. Phys.* **37**, L398 (1998).